Prepublished Copy

NATURE ENVIRONMENT AND POLLUTION TECHNOLOGY

Article In Press

PEER-REVIEWED PREPUBLISHED MANUSCRIPT

This is a peer-reviewed prepublished version of the paper to be published in **Vol. 26, No. 1, March 2027.**

Deciphering the Bioremediation Potential and Plant Growth-Promoting Traits of a Soil-Derived Isolate Pantoea dispersa MS 3: From Spectroscopic Characterization to Phytotoxicity Assessment

Mohini Pimpalse and Naga Rathna Supriya G.

RECEIVED
23 May 2026

CITE THIS ARTICLE

Pimpalse, M. and Naga Rathna Supriya G., 2027. Deciphering the Bioremediation Potential and Plant Growth-Promoting Traits of a Soil-Derived Isolate Pantoea dispersa MS 3: From Spectroscopic Characterization to Phytotoxicity Assessment. Nature Environment and Pollution Technology, 26(1), B4455.

https://doi.org/10.46488/NEPT.2027.v26i01.B4455

EARLY-ACCESS STATEMENT

This manuscript, after peer review, is being released online in its original, unedited form to provide early access to its findings. Prior to final publication, it will undergo additional editing and formatting. Readers may note that, as an unedited version, the manuscript may have linguistic and other minor errors. The DOI will be active after the final publication of the paper.

PUBLICATION STATUS

PEER REVIEW	ONLINE VERSION	FINAL ISSUE
Completed	**Prepublished**	**March 2027**

Deciphering the Bioremediation Potential and Plant Growth-Promoting Traits of a Soil-Derived Isolate *Pantoea dispersa* MS 3: From Spectroscopic Characterization to Phytotoxicity Assessment

Mohini Pimpalse and Naga Rathna Supriya G.*

C. G. Bhakta Institute of Biotechnology, Uka Tarsadia University, Maliba Campus, Bardoli, Gujarat, India
Corresponding Author:

Dr. Naga Rathna Supriya G

Email: rathna.supriya@utu.ac.in

Phone: 8141109956

ORCID: 0000-0001-7410-2905

Abstract

Textile industry effluents containing synthetic azo dyes pose a severe threat to environmental and soil health due to their recalcitrant and toxic nature, leading to inhibition of aquatic photosynthesis, depletion of dissolved oxygen, reduction of soil fertility, and the formation of toxic, carcinogenic aromatic amines that bioaccumulate through the food chain. This study aimed to isolate and characterize a multifunctional bacterial strain capable of both azo dye decolorization and plant growth promotion. Among fifteen soil isolates, strain MS 3 was selected for its superior performance and identified as *Pantoea dispersa* MS 3 (GenBank OP303250). Quantitative assays demonstrated that MS 3 showed significant decolorization efficiencies for three structurally diverse dyes, namely Dk. Red RB (90.5%), Blue GSL (89.6%), and a peak efficiency of 92.07% for Scarlet RR. Analytical evaluation using UV-Vis, TLC, and FTIR indicated structural transformation of the parent dye molecules following bacterial treatment, supporting azo dye decolorization. Furthermore, *P. dispersa* MS 3 exhibited robust PGP attributes, including N_2 fixation, phosphate solubilization (20.26 µg/mL), and the production of IAA (44.74 µg/mL), a siderophore (68.6% SU), and gibberellic acid (111.17 µg/mL). A phytotoxicity study using *Vigna radiata* L. revealed that bacterial treatment significantly mitigated dye-induced stress, increasing germination rates from 40% in dye-polluted controls to 73.3% in treated samples and enhancing seedling vigor. These findings demonstrated that *P. dispersa* MS 3 exhibited promising azo dye decolorization and plant growth-promoting characteristics under controlled laboratory conditions, highlighting its potential for future bioremediation applications. This study demonstrates the multifunctional potential of a dye-contaminated soil-derived *P. dispersa* MS 3 exhibiting both azo dye decolorization and plant growth-promoting characteristics under laboratory conditions.

Keywords: Dye degradation, *Pantoea dispersa,* PGP, TLC, FTIR, Phytotoxicity

Introduction

The textile industry is a primary contributor to global environmental pollution, discharging vast quantities of wastewater laden with recalcitrant synthetic dyes, heavy metals and persistent salt (Ikram et al. 2022a; Pandey et al. 2024). Among these, azo dyes are of significant concern due to their complex aromatic structure, high stability and resistance to conventional treatment processes (Pandey et al. 2024; Shahid et al. 2018). Azo dyes are the largest class of synthetic colorants, characterized by the presence of one or more nitrogen-to-nitrogen double bonds (–N=N–) that link complex aromatic ring structures into a conjugated system (Zafar, Bukhari, and Rehman 2022). Their improper discharge into water bodies creates a destructive barrier that hinders light penetration and reduces dissolved oxygen, severely impacting the photosynthetic activity of aquatic flora and the survival of fauna (Ikram et al. 2022b; Kishor, Purchase, et al. 2021a). In agricultural region, the use of this contaminated water for irrigation poses additional risks to soil health, microbial communities and crop productivity (Kishor, Purchase, et al. 2021a; Shahid et al. 2018).

Conventional dye remediation methods such as coagulation, adsorption and advanced oxidation processes are widely used. However, biological methods are increasingly preferred due to their cost-effectiveness, eco-friendly nature and lower generation of secondary pollutants (Ikram et al. 2022a). Among them, bacterial-mediated remediation has great advantages for its rapid growth, great environmental adaptability and amazing metabolic versatility that enable efficient degradation and mineralization of azo dyes into less toxic compounds (Barua et al. 2023; Suhag et al. 2021). Due to their fast growth rates, biochemical versatility, and ability to adapt to extreme environmental conditions, bacterial systems are particularly efficient for bioremediation (Meerbergen et al. 2018a; Pandey et al. 2024). Microorganisms transform complex dye molecules into simpler, non-toxic metabolites by reductively cleaving azo bonds (-N=N-) using enzyme systems including azoreductases, laccases, and peroxidases (Ikram et al. 2022a; Pandey et al. 2024; Srinivasan and Sadasivam 2018).

A multifunctional bacterial strain with dye degradation capability and plant growth promotion (PGP) abilities is being increasingly sought out in modern research (Shahid et al. 2018). In contaminated soils, these bacteria are often isolated from harsh rhizospheres of plants, providing plants with resilience against anthropogenic stresses. These beneficial microbes employ direct mechanism such as biological nitrogen fixation, phosphate solubilization, and the production of siderophore to enhance nutrient availability (Rani et al. 2025). Furthermore, they synthesize essential phytohormones, including Indole -3-acetic acid, and Gibberellic acid (GA3), which stimulate root development and compensate for hormone loss induced by environmental stress.

The primary objective of this study is to screen and isolate indigenous bacteria from dye-contaminated soil that exhibit high potential for dye degradation. This investigation aims to identify the most potent isolate and analyze the biochemical pathways of degradation through UV-Vis, TLC, and FTIR. Furthermore, the multifarious PGP activities of the isolate, including N2 fixation, phosphate solubilization, and the production of gibberellic acid, siderophores, and IAA, will be characterized. Finally, the study will assess the phytotoxicity of the degraded metabolites to

determine their impact on germination and growth inhibition, providing a sustainable framework for industrial effluent treatment.

Materials and Methodology

Materials

The dyes used in this experiment Dk. Red RB ($C_{14}H_{15}N_3$), Blue GSL ($C_{34}H_{24}N_6Na_4O_{16}S_4$) and Scarlet RR ($C_{18}H_{18}BrN_5O_7$) were obtained as generous gift from the textile industry, Surat-Gujarat. All the media that are used in this study was from Hi-media.

Sample collection and Isolation

The soil sample was collected from dye-contaminated area within the premises of a textile manufacturing unit located in Sachin - Surat, Gujarat, India. Sampling was performed at a depth of 25-30 cm. The collected soil sample was serially diluted (10^{-1} to 10^{-7}), aliquot of dilution was aseptically spread on a petri plate containing nutrient agar (peptone- 5.0 g/L, beef extract- 3.0 g/L, sodium chloride- 5.0 g/L, and agar- 15.0 g/L; pH 7.0±0.2) amended with 100 ppm of three different azo dye (Dk. Red RB, Blue GSL and Scarlet RR), and incubated at 37˚ C for 24–48 hrs(Biruntha et al. 2021). The distinct bacterial colonies which exhibit clear zone were isolated and maintained on a nutrient agar slant at 4°C for further experiments.

Dye decolorization assay

The isolated bacterial strains were inoculated in 100 mL of nutrient broth in a 250 mL flask supplemented with azo dye, namely Dk. Red RB, Blue GSL and Scarlet RR at the concentration of 100 ppm. A bacterial inoculum volume of 5 mL was added to the nutrient broth and incubated at 37˚C under static conditions. The decolorized sample was withdrawn at 24-hour intervals and OD was measured at the respective λmax of the dyes (510 nm for Dk. Red RR, 620 nm for Blue GSL and 520 nm for Scarlet RR). The nutrient broth supplemented with the respective dyes without bacterial inoculum was set as the control (Khan, Nayarisseri, and Singh 2025). All experiments were performed in triplicate.

$$Decolorization\ (\%) = \frac{Initial\ Absorbance - Final\ Absorbance}{(Initial\ Absorbance)} \times 100$$

Molecular identification

The genomic DNA of the bacterial strain with the highest decolorization efficiency among the three azo dyes was extracted using the CTAB method (Chachaty and Saulnier 2000). The strain was identified through 16S rRNA gene sequencing using universal primers 27F and 1492R at SLS Research Pvt Ltd., Surat, Gujarat-India. The obtained sequence was analyzed using the Basic Local Alignment Search Tool (BLAST) on the National Center for Biotechnology Information (NCBI) database. Following the submission of the nucleotide sequence to GenBank, an accession number was assigned and submitted.

Analytical analysis

Extraction of metabolites

The decolorized samples of Dk. Red RB, Blue GSL, and Scarlet RR were centrifuged at 10,000 rpm for 20 minutes at room temperature, and the obtained supernatants were subjected to metabolite extraction. Each sample was extracted three times with an equal volume of ethyl acetate including the control sample (uninoculated dye). The extracts were dried over anhydrous Na_2SO_4 and concentrated to dryness using a rotary evaporator. The dried residues were dissolved in a small volume of HPLC grade methanol and analysed using UV-Vis spectral analysis, TLC, and FTIR to investigate the decolorization and degradation process (Pandey et al. 2024).

UV-Vis Spectral Analysis

The decolorized products generated by the selected isolates and untreated control dye were analyzed by monitoring changes in the UV-Vis spectra between the range 300-800 nm using a Shimadzu UV-1900i spectrophotometer. The spectral shift changes in driven by bacteria in all three azo dyes were observed (Meerbergen et al. 2018b).

Thin Layer Chromatography (TLC)

Thin Layer Chromatography was performed on silica gel to analyze the degradation product resulting from the biodegradation of Dk. Red RB, Blue GSL, and Scarlet RR azo dyes. The mobile phase was used in combination with n-hexane and dichloromethane (3:7). Extracted metabolites from bacterial treated and control were spotted on the TLC plates. The spot detection was carried out by placing the developed chromatograms in an iodine chamber, followed by observation under visible light (Ajaz et al. 2019a).

Fourier Transform Infrared Spectroscopy (FTIR)

Fourier Transform Infrared Spectroscopy analysis was performed of the extracted metabolites of the control dye and their respective biodegradation products to identify the structural change of the dye before and after decolorization. The mid-infra range of 400–4000/cm was where the FTIR study was conducted. The Bruker Optics Alpha II-ATR spectrophotometer was used to conduct experiments in the 400–4000 cm^{-1} mid-infrared range at a 16-scan speed (Srinivasan and Sadasivam 2021).

Plant Growth Promoting Traits

N_2 Fixation

An experiment to determine the bacteria's ability to fix N_2 was conducted by streaking a loopful of 24-h culture on Jensen agar medium (sucrose- 2g; K_2HPO_4- 01.g; $MgSO_4$- 5 mg; NaCl-5 mg; $FeSO_4$- 1 mg; Na_2MoO_4- 0.5 mg; $CaCO_3$-0.2 g; Agar-1.5 g; d.H_2O-100 mL). N_2 fixation was qualitatively evaluated by the appearance of bacterial growth on Jensen agar plates (Jensen 1955; Wael et al. 2024).

Phosphate solubilization

Phosphate solubilization ability of the bacterial isolate was assessed using Pikovskaya's agar medium (yeast extract 0.5 g/L, dextrose 10 g/L, calcium phosphate 5 g/L, potassium chloride 0.2 g/L, ammonium sulphate 0.5 g/L, magnesium sulphate 0.1 g/L, manganese sulphate 0.0001 g/L, ferrous sulphate 0.0001 g/L, agar 15 g/L). Following incubation at 30°C for 24-72 hours, the formation of a clear halo zone around the bacterial colony was observed.

The phosphate solubilization index (PSI) was calculated based on the halo zone and colony diameter. For quantitative analysis, National Botanical Research Institute's phosphate (NBRIP) broth was used. The experiment was conducted 100 mL Erlenmeyer flask containing 20 mL of NBRIP medium, inoculated with the bacterial isolate, while uninoculated sterile medium served as a negative control. Flask was incubated at 30°C for 48 hours at 100 rpm in a shaking incubator. After incubation, culture was centrifuged at 10,000 rpm for 10 minutes, and the soluble phosphate concentration in the supernatant was determined by measuring absorbance at 410 nm using a spectrophotometer. A standard calibration curve was prepared using known concentration of potassium dihydrogen phosphate (KH_2PO_4) (Amri et al. 2023; Nautiyal 1999).

Indole-3-Acetic Acid Production

IAA production was assessed following the method of Gordon & Paleg 1957 (Gordon and Paleg 1957). Bacterial cultures were inoculated in nutrient broth supplemented with tryptophan (5 µg/mL) and incubated at 35°C for 5 days. After incubation, cultures were centrifuged at 3,000 rpm for 10 min. To 2 mL of the supernatant, two drops of orthophosphoric acid and 4 mL of Salkowski's reagent (50 mL 35% perchloric acid, 1 mL 0.5% $FeCl_3$) were added and incubated for 30 min in the dark at room temperature. The appearance of a red color indicated a positive result. The density of pink was measured by a spectrophotometer with wavelength 530 nm (Joshi, Kumar, and Brahmachari 2021).

Siderophore production

Siderophore production was qualitatively evaluated using Chrome Azurol S (CAS) agar medium (Grimm and Allen 1954). Isolates were streaked onto CAS agar plates and incubated at room temperature for 2 to 4 days. The formation of orange halos around the colonies indicated siderophore production. The assay was performed in duplicate. The quantitative assessment of siderophore production was performed using the CAS-shuttle assay as described by (Schwyn and Neilands 1987). Cultures were grown in sterile succinate broth, and siderophore production was quantified as Percentage Siderophore Unit (% S.U) using the formula as below (Kalyan et al. 2022).

$$\%S.U = \frac{Ar - As}{Ar} \times 100$$

where Ar is the absorbance of the reference (uninoculated medium + CAS assay solution) and As is the absorbance of the sample (cell-free supernatant + CAS assay solution).

Gibberellic Acid (GA_3)

GA3 was estimated calorimetrically using the standard procedure proposed by Holbrook et al. (1961) (HOLBROOK, EDGE, and BAILEY 1961) with slight modifications. Bacterial isolates were inoculated in nutrient broth and incubated at 28±2°C for 24 hours. After incubation, cultures were centrifuged at 10,000 rpm for 15 minutes at room temperature. 2 mL zinc acetate reagent was mixed to 15 mL supernatant and incubated for 2 minutes followed by addition 2 mL 10.6% potassium ferrocyanide and the resulted mixture was centrifuged at 2000 rpm for 15 minutes. Supernatant and 30% hydrochloric acid (HCl) were mixed in equal volume and incubated at 20°C for 75 minutes. After incubation absorbance was measured at 254 nm, and the concentration of gibberellins was calibrated using

gibberellic acid (100-1000ug/ml) standard curve. 5 mL of 5% HCl was used as a blank solution (Sharma 2018). All plant growth-promoting assays, both qualitative and quantitative, were performed in triplicate.

Phytotoxicity Assessment of decolorized product

Vigna radiata L. seeds were used for the phytotoxicity assessment due to their rapid germination, high sensitivity to environmental contaminants, and widespread use as a model plant in phytotoxicity studies.

A comparison of untreated dye, bacterial decolorized product, and a water control were made in order to determine their effects on seed germination and early seedling development. A 2.0% $HgCl_2$ surface sterilization procedure was carried out to eliminate fungal contamination on seeds of *V. radiata* L., and the seeds were subsequently rinsed with sterile distilled water. The seeds were placed in sterile Petri dishes lining with Whatman No. 1 filter paper and irrigated with untreated dye, bacterial decolorized product, and a water control. Each treatment consisted of three independent replicates. A percentage of seed germination was measured after two days and roots and shoots after seven days of incubation. The germination percentage of seeds was calculated using the following formula (Kishor, Purchase, et al. 2021b):

$$Germination\ (\%) = \frac{No.of\ germinated\ seeds}{No.of\ sowed\ seeds} \times 100$$

$$Inhibition\ (\%) = \frac{(No.of\ seeds\ germinated\ in\ control - No.of\ seeds\ germinated\ in\ treatment)}{No.of\ seeds\ germinated\ in\ control} \times 100$$

Statistical analysis

All experiments were performed in triplicate, and data are expressed as mean ± standard deviation (SD). Statistical significance between treatments was assessed with a one-way ANOVA, followed by Tukey's HSD post hoc test at $p < 0.05$. Means sharing different lowercase letters within the same column show a statistically significant difference.

Results

Sample collection and Isolation

A total of 15 morphologically distinct bacterial colonies were isolated from the textile contaminated soil sample under the employed screening condition and coded as MS 1 to MS 15. Upon preliminary evaluation on solid media supplemented with the selected textile azo dye (Dk. Red RB, Blue GSL and Scarlet RR), five of these isolates exhibited pronounced clear zones surrounding the colonies (MS 1, MS 2, MS 3, MS 8 and MS 14), indicating their potential dye decolorization or degradation capability. These five isolates were selected for subsequent quantitative dye decolorization assay to rigorously assess their efficiency in biotransformation and decolorization under controlled laboratory conditions.

Dye decolorization assay

Based on preliminary screening of dye degradation activity, five promising bacterial isolates, namely MS 1, MS 2, MS 3, MS 8, and MS 14, demonstrated prominent clear zones around the colonies were selected for quantitative dye decolorization assay with 3 different dyes (Dk. Red RB, Blue GSL, and Scarlet RR). The dye degradation assay

revealed significant variability among the isolates in their capacity to degrade the dyes, indicating strain-specific enzymatic potential and dye substrate specificity. Among all isolates, MS 3 demonstrated the highest decolorization, achieving 90.5% (±0.07) for Dk. Red RB, 89.6% (±0.4) for Blue GSL, and 92.07% (±0.1) for Scarlet RR (Figure 1). Isolates MS 1 and MS 2 also showed substantial decolorization potentials, with efficiencies in the range of 67-80%. In contrast, MS 8 demonstrated minimal decolorization activity (<36%), suggesting a limited adaptive mechanisms or enzymatic capacity to metabolize the selected dyes. While MS 14 showed moderate decolorization activity against all azo dyes.

Figure 1. Comparative decolorization of Dk. Red RB, Blue GSL, Scarlet RR by selected bacterial isolates

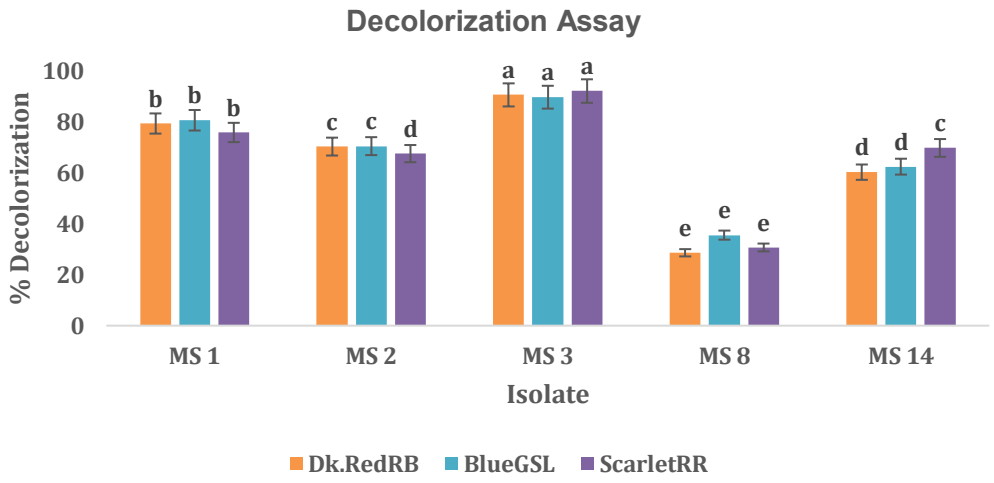

Decolorization efficiency (%) of selected bacterial isolates (MS 1, MS2, MS 3, MS 8 and MS 14), with MS 3 exhibiting the efficient dye decolorization, against three textile dyes namely Dk. Red RB, Blue GSL, Scarlet RR. One-way ANOVA was performed; the bars and different letters are showing standard deviation and significant difference at $p < 0.05$ according to Tukey's HSD test, respectively.

Molecular identification

The most efficient dye-decolorizing isolate MS 3 was subjected to molecular identification through 16S rRNA gene sequencing. Genomic DNA was extracted using CTAB method (Chachaty and Saulnier 2000). The 16S rRNA gene was amplified using universal bacterial primers 27F and 1492R under standardized PCR conditions (initial denaturation at 95˚C - 5 min, 35 cycles for 95˚C - 1 min, 55˚C - 1 min, 72˚C - 1.5 min, and final extension at 72˚C - 10 min) (Weisburg et al. 1991). The amplified product was sequenced, and the resulting sequence was analysed using BLASTN against the NCBI nucleotide database. Based on sequence similarity and phylogenetic analysis, isolate MS 3 was identified as *Pantoea dispersa* (Figure 2). The 16S rRNA gene sequence was submitted to the NCBI GenBank database and assigned an accession number OP303250.

Figure 2. Molecular phylogenetic analysis of *Pantoea dispersa* strain MS 3 using 16S rRNA gene sequence analysis

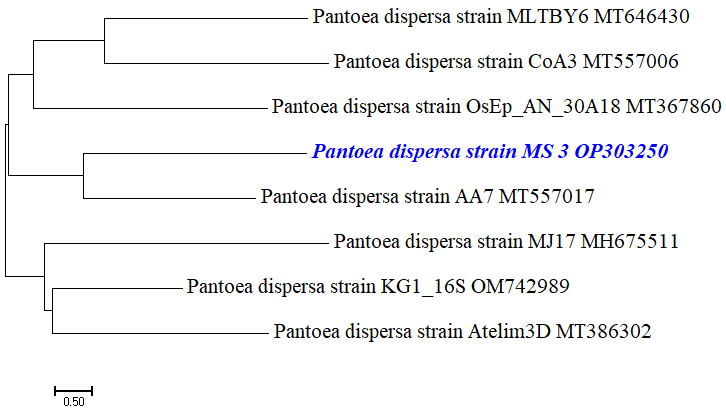

The phylogenetic tree showing the evolutionary relationship of *Pantoea dispersa* MS 3 strain (OP303250) with closely related *Pantoea dispersa* strains based on 16S rRNA gene sequence homology obtained from the NCBI database.

Analytical analysis

To confirm the structural transformation of azo dyes by the selected isolate *P. dispersa* MS 3, analytical techniques including UV-Vis spectrophotometry, TLC and FTIR were employed. The results revealed significant transformation of the azo dye molecules by *P. dispersa* MS 3, indicating effective biodegradation mechanism.

UV-Vis Spectral Analysis

The UV-Vis spectroscopic profile obtained in the present investigation provide compelling evidence for the efficient transformation of structurally distinct azo dyes, namely Dk. Red RB, Blue GSL and Scarlet RR, mediated by *P. dispersa* MS 3. The untreated dye Dk. Red RB, Blue GSL and Scarlet RR exhibited intense and well-defined absorption peaks within the visible region, corresponding to their respective chromophoric azo groups. A strong absorption peak observed for Dk. Red RB at λmax~510, Blue GSL at λmax~620 and Scarlet RR at λmax~520 nm. Following microbial treatment with *P. dispersa* MS 3, a substantial reduction in peak intensity was noted across all dyes, indicating the disruption of the azo bond (-N=N-) and supporting effective decolorization (Figure 3).

Figure 3: UV-Vis Spectral changes indicating decolorization of Dk. Red RB (2a), Blue GSL (2b), and Scarlet RR (2c) by *P. dispersa* MS 3

3a

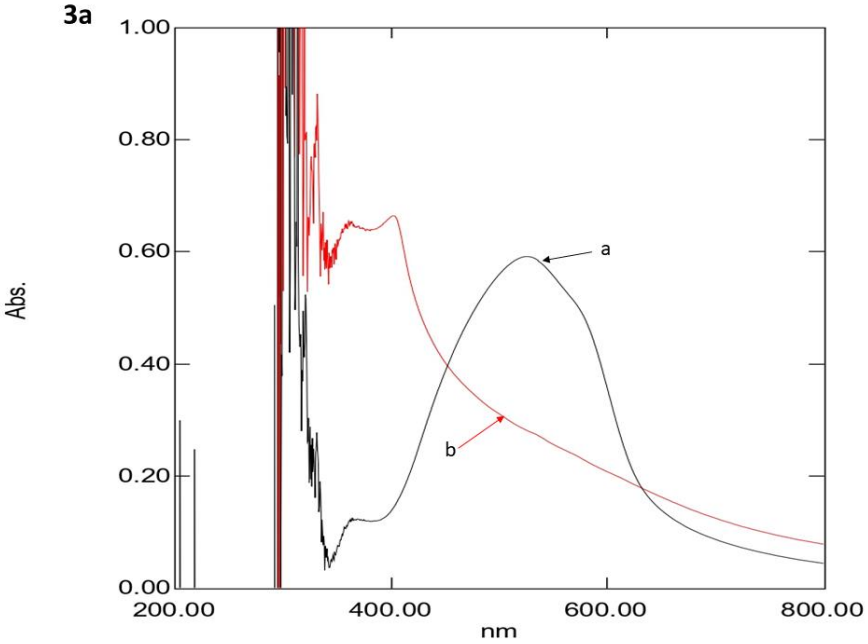
1.00
0.80
0.60
0.40
0.20
0.00
Abs.
200.00
400.00
600.00
800.00
nm
a
b

3b

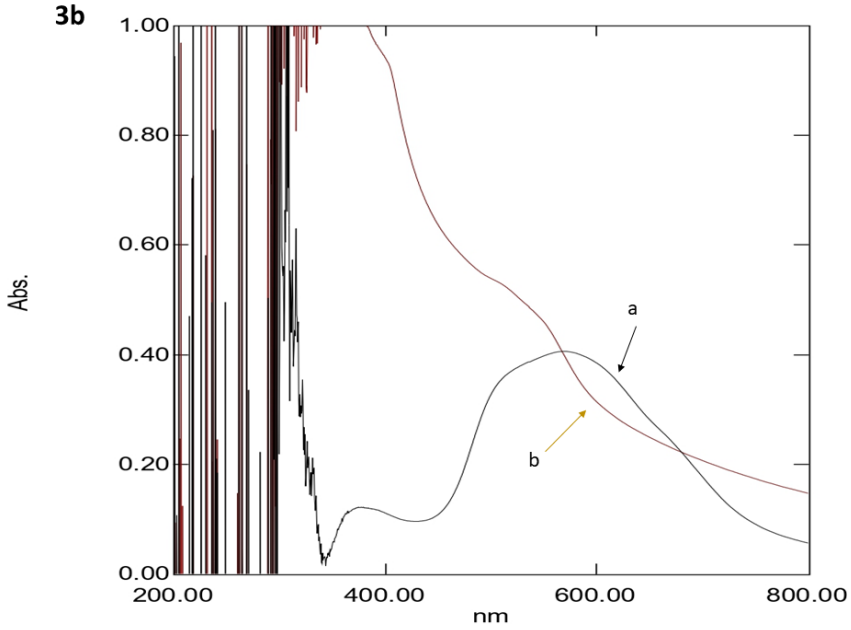
1.00
0.80
0.60
0.40
0.20
0.00
Abs.
200.00
400.00
600.00
800.00
nm
a
b

3c

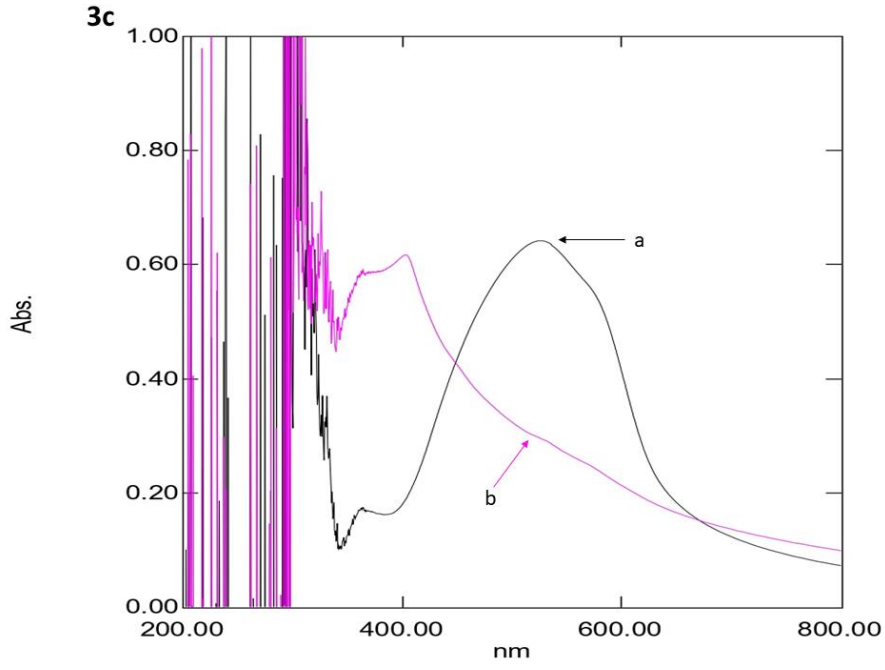
1.00
0.80
0.60
0.40
0.20
0.00
Abs.
200.00
400.00
600.00
800.00
nm
a
b

In each graph, an examination of the UV–Vis spectra of dyes before (a) and after (b) treatments with *P. dispersa* MS3, indicated dye degradation by a reduction in absorbance; (2a) Dark Red RB, (2b) Blue GSL, and (2c) Scarlet RR.

Thin Layer Chromatography (TLC)

TLC is widely used to verify the structural transformation of azo dyes after bacterial treatment by comparing chromatographic banding patterns of untreated and treated samples. In the control sample (untreated original dye), each azo dye exhibited a single prominent band, indicating the presence of the intact parent compound, with Rf values of 0.32, 0.88, and 0.95 of Dk. Red RB, Blue GSL, and Scarlet RR, respectively. The emergence of multiple distinct bands in the treated samples after bacterial treatment indicated structural transformation of the original parent dye molecules and the formation of transformation products with different chromatographic mobilities. A total of six distinct bands were observed in the Dk. Red RB samples with Rf values of 0.15, 0.29, 0.39, 0.44, 0.61, and 0.93 (Figure 4a), suggesting the formation of multiple transformed products with varying polarity. Decolourized samples of Blue GSL showed five bands with Rf values of 0.10, 0.48, 0.65, 0.70, and 0.88 (Figure 4b), while treatment of Scarlet RR resulted in six bands with Rf values of 0.12, 0.30, 0.65, 0.77, 0.88, and 0.93 (Figure 4c).

Figure 4: TLC analysis of azo dyes (Dk. Red RB, Blue GSL and Scarlet RR) before and after biodegradation by *P. dispersa* MS 3

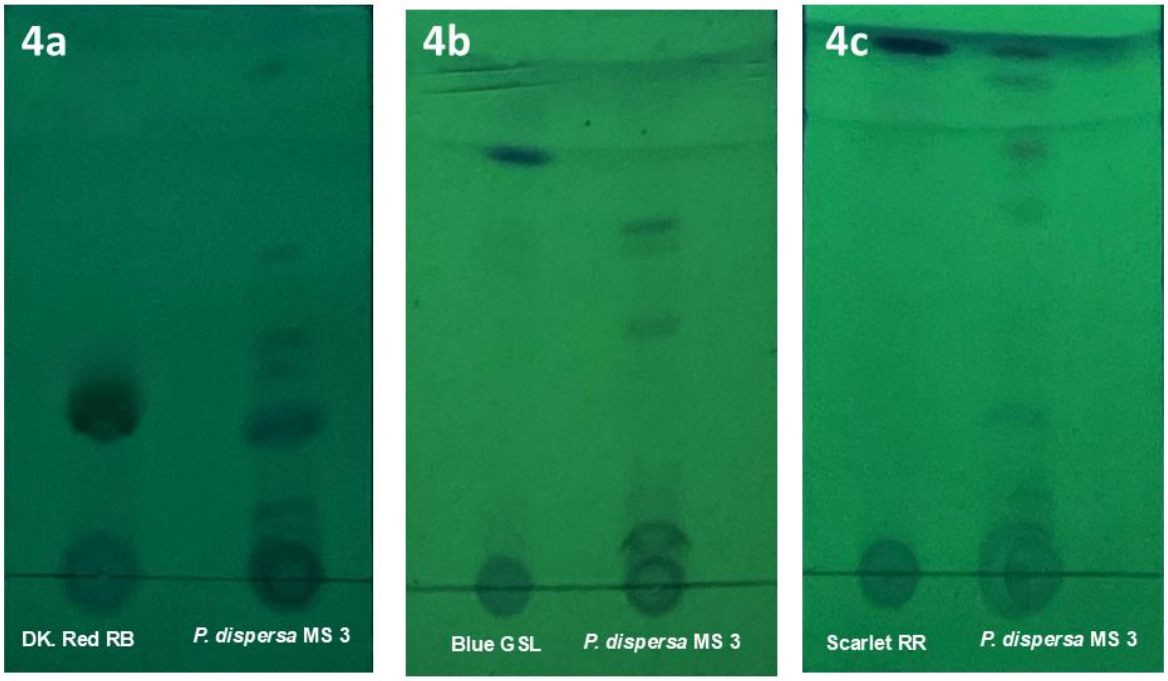

In each TLC image, the left lane is the control dye sample with a single band (a: Dk. Red RB, b: Blue GSL, c: Scarlet RR), and the right lane is the bacterial-treated sample with multiple bands, indicating azo dye breakdown and formation of metabolites

Fourier Transform Infrared Spectroscopy (FTIR)

Fourier-Transform Infrared Spectroscopy (FTIR) was employed to elucidate structural modification in azo dyes (Dk Red RB, Blue GSL, and Scarlet RR) following biotransformation by *P. dispersa* MS3. Significant shifts, reductions, or disappearances in key absorption bands were found in the comparison spectra, indicating biotransformation of the parent dye molecules (Table 1). Untreated azo dyes showed characteristic absorption band around 1650 cm^{-1} along with other peaks corresponding to aromatic, sulfonic, and amine functional groups (Figure 5). Given that the 1650 cm^{-1} spectral region may correspond to overlapping vibrational modes of various functional groups, peak assignments were interpreted in conjunction with UV–Vis and TLC analyses. Additional characteristic bands were detected in regions associated with the stretching vibrations of OH, N-H, and C-N, which is consistent with the molecular structure of the dye. Following bacterial treatment, noticeable shifts and changes in the intensity of absorption bands were observed, suggesting structural transformation of the dye molecules. The region of aromatic amines, sulfonates, and hydroxyl groups showed further spectral changes which indicated the transformation of complex dye molecules into simpler molecules.

Table 1. Comparison of characteristic FTIR absorption bands between untreated and treated azo dye samples with *Pantoea dispersa* MS 3.

Dye	Control FTIR peak (cm^{-1})	Treated FTIR peak (cm^{-1})	Observation
Dk. Red RB	1650	1658	Peak shift with reduced intensity observed
Blue GSL	1650	1637	Peak shift with reduced intensity observed
Scarlet RR	1650	1655	Peak shift with reduced intensity observed

Values represent the characteristics of the absorption band observed around 1650 cm-1 in untreated and bacterial-treated dye samples. The absorption band in this region may represent overlapping contributions from azo chromophore-associated vibrations and other functional groups.

Figure 5: FTIR analysis of azo dyes (Dk. Red RB, Blue GSL, and Scarlet RR) before and after decolorization by *P. dispersa* MS 3

5a

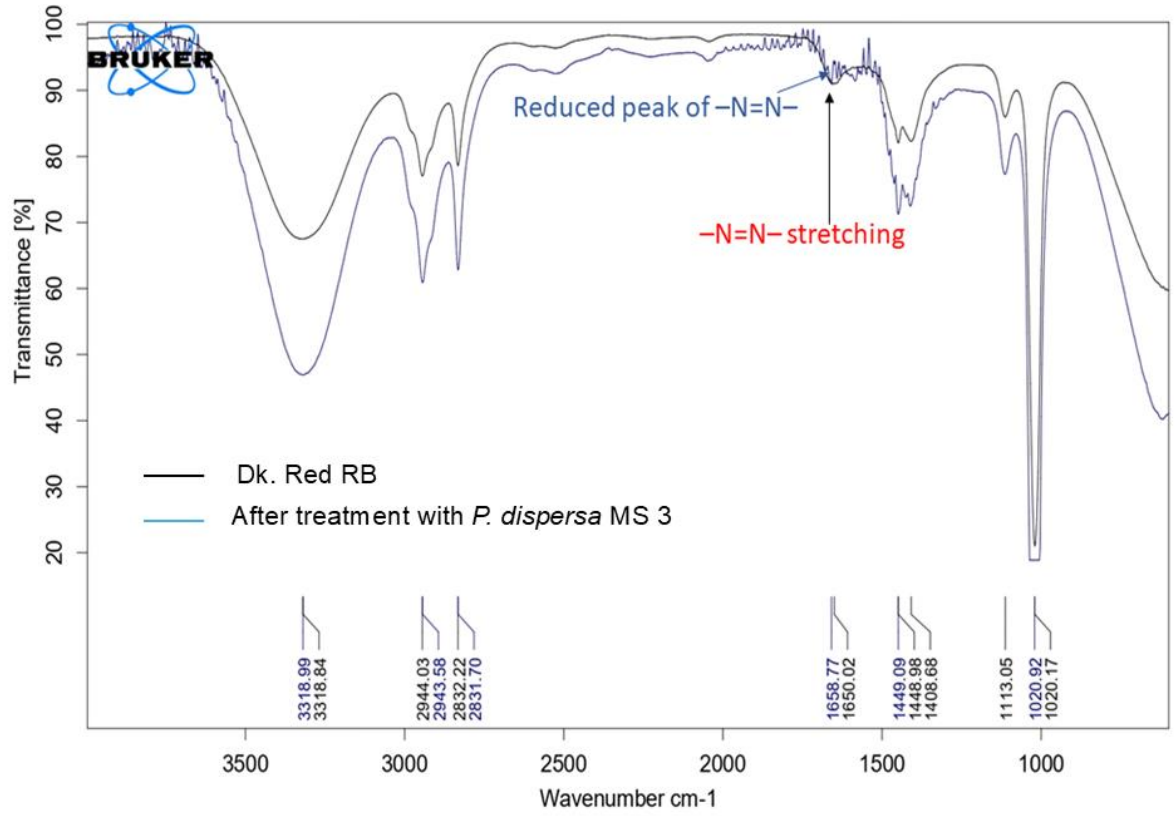
BRUKER
Reduced peak of –N=N–
–N=N– stretching
Transmittance [%]
Dk. Red RB
After treatment with P. dispersa MS 3
3318.99
3318.84
2944.03
2943.58
2832.22
2831.70
1658.77
1650.02
1449.09
1448.98
1408.68
1113.05
1020.92
1020.17
Wavenumber cm-1

5b

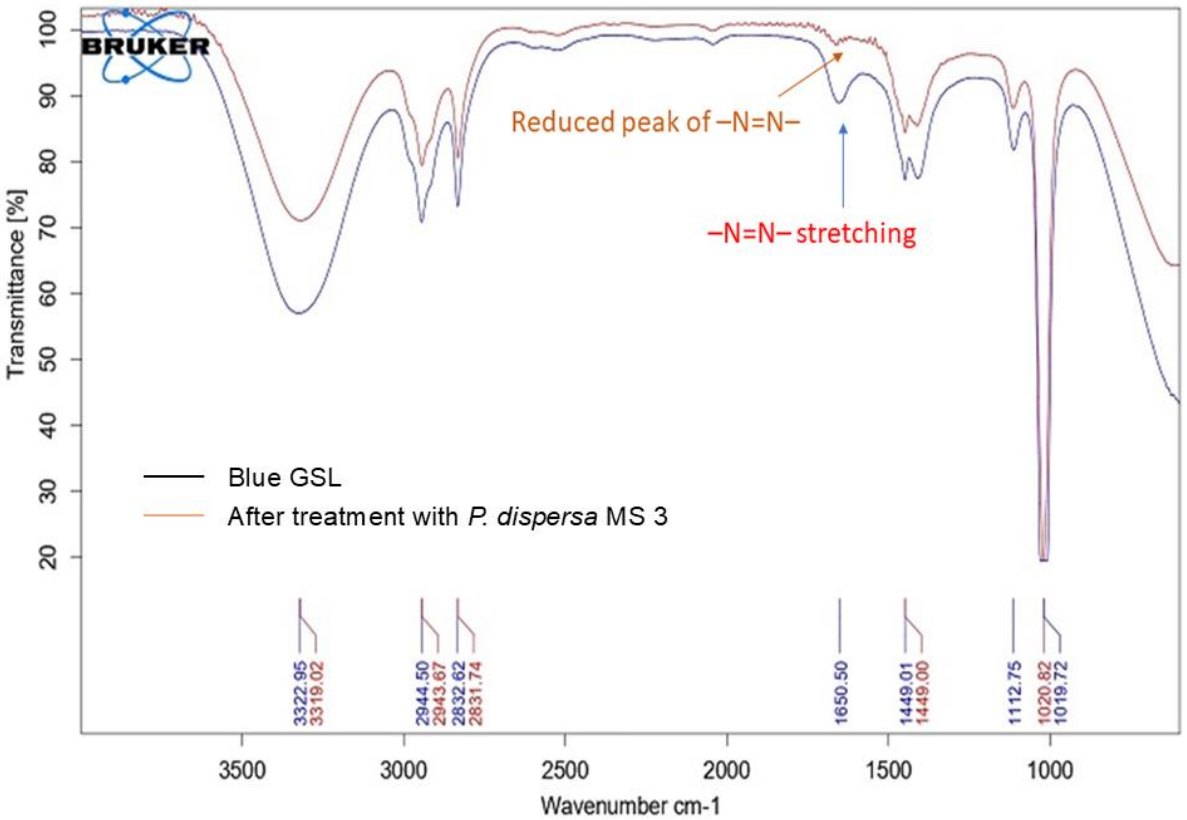
BRUKER
Reduced peak of –N=N–
–N=N– stretching
Transmittance [%]
Blue GSL
After treatment with P. dispersa MS 3
3322.95
3319.02
2944.50
2943.67
2832.62
2831.74
1650.50
1449.01
1449.00
1112.75
1020.82
1019.72
Wavenumber cm-1

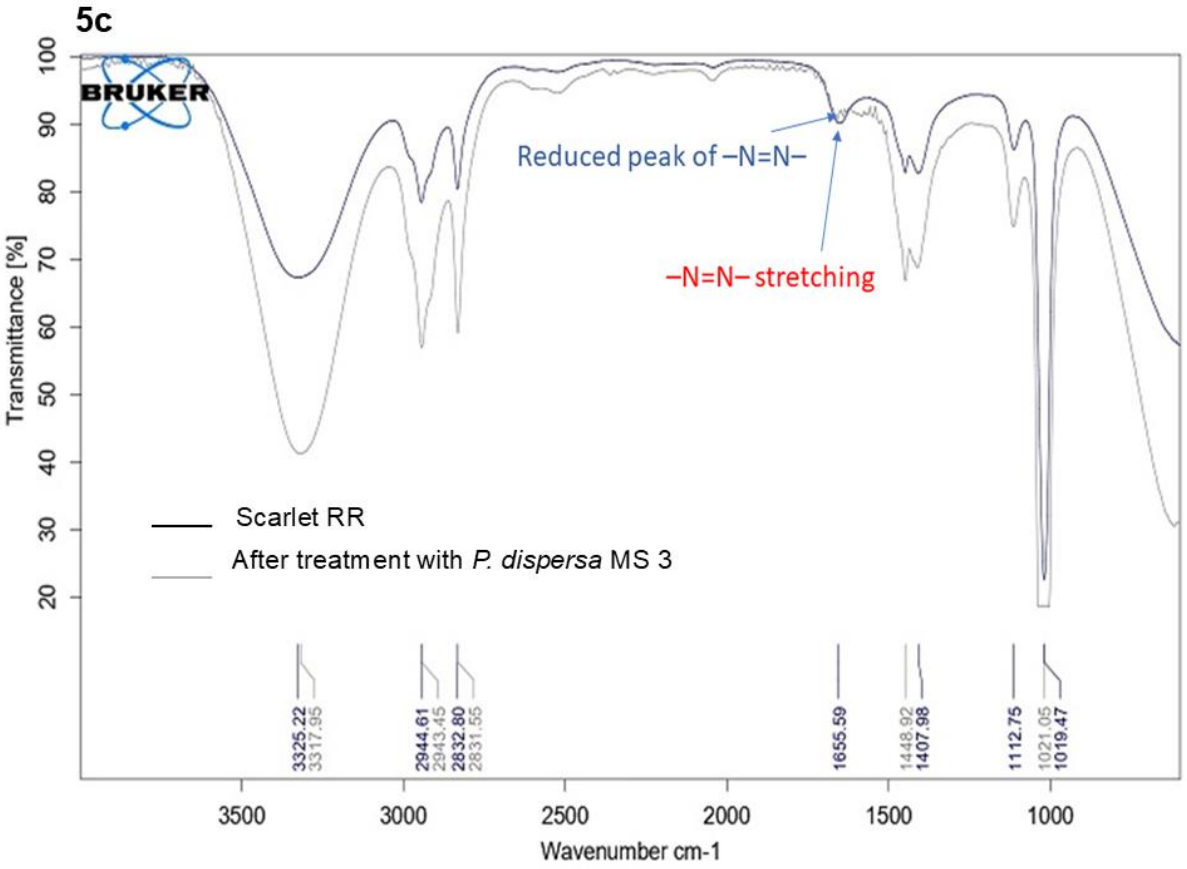

Plant Growth-Promoting Traits

To assess the potential of *P. dispersa* strain MS3 as a bioinoculant, multiple plant growth-promoting (PGP) traits were evaluated. A positive result was achieved across all types of parameters measured, including nitrogen fixation, IAA production, siderophore production, phosphate solubilization, and gibberellic acid production.

N_2 Fixation

Pantoea dispersa MS3 was preliminarily assessed for N_2 fixation potential on nitrogen-free Jensen medium. Visible growth indicated putative diazotrophic capability and the potential to utilize atmospheric N_2 as the sole nitrogen source.

Phosphate solubilization

The Phosphate solubilization index (PSI) of *P. dispersa* MS3 on Pikovskaya's agar was 1.42, showing a 6 mm zone of solubilization around colonies. The quantitative analysis demonstrated the soluble phosphate concentration was 20.26 (±0.21) µg/mL.

Indole-3-Acetic Acid Production

Qualitative analysis of *Pantoea dispersa* MS 3 showed development of a characteristic pink coloration after the addition of Salkowski reagent, indicating IAA production. Further quantitative estimation revealed IAA production of 44.74 (± 0.94) µg/mL.

Siderophore production

Pantoea dispersa MS3 showed a clear orange halo of 9 mm on CAS agar, indicating siderophore secretion under iron-limited conditions. Quantitative estimation showed consistently high siderophore production, 68.6 (±0.20) %SU.

Gibberellic Acid (GA_3)

Gibberellins are vital hormones in plants which govern stem elongation and seed germination. In the present study, GA_3 production by *P. dispersa* MS 3 was recorded at 111.17 (±0.04) µg/mL.

Phytotoxicity assessment of decolorized product

The phytotoxicity study conducted using *Vigna radiata* L. seeds demonstrated the adverse effects of the azo dyes on seed germination and seedling growth parameters. The water control exhibited 100% germination and recorded the highest root and shoot lengths among all treatments. In contrast, the dye control significantly reduced germination percentages to 43.3%, 46.6%, and 40% in Dk. Red RB, Blue GSL, and Scarlet RR treatment, respectively. Correspondingly, germination inhibition was increased to 56.7%, 53.3%, and 60% due to azo dye Dk. Red RB, Blue GSL, and Scarlet RR treatments, respectively (Table 2). A considerable decline in seedling growth was also observed under dye stress conditions. In the dye control, root lengths decreased to 1.23 (±0.04), 2.46 (±0.02), 2.56 (±0.11) cm, while shoot lengths were reduced to 1.64 (±0.04), 4.15 (±0.04), 2.03 (±0.15) cm in Dk. Red RB, Blue GSL, and Scarlet RR, respectively, compared to water control.

Table 2. The phytotoxic effect of decolorized dye product by *Pantoea dispersa* MS 3 on seed germination and inhibition percentage of *Vigna radiata* L. under azo dye stress conditions

Treatment	Dk Red RB	Blue GSL	Scarlet RR
Germination (%)			
Water Control	100[a]	100[a]	100[a]
Dye Control	43.3[c]	46.6[c]	40[c]
Pantoea dispersa MS 3	63.3[b]	63.3[b]	73.3[b]
Inhibition (%)			
Water Control	0	0	0
Dye Control	56.7	53.3	60
Pantoea dispersa MS 3	36.7	36.7	26.7

Values represent the mean seed germination percentage and inhibition percentage of *V. radiata* L. under water control, dye control, and bacterial treatment using DK. Red RB, Blue GSL, Scarlet RR dyes. Different alphabetic letters within the same column show significant differences ($p < 0.05$) according to Tukey's HSD test following one-way ANOVA.

Treatment with *Pantoea dispersa* MS3 significantly alleviated dye-induced phytotoxicity and improved seed germination as well as seedling growth. In Dk. Red RB, Blue GSL, and Scarlet RR treatments, germination percentages increased to 63.3%, 63.3%, and 73.3%, respectively, while corresponding inhibition percentages decreased to 36.7%, 36.7%, and 26.7%. Additionally, under azo dye-stressed conditions, shoot lengths increased to 2.66 ± 0.15 cm, 6.63 ± 0.25 cm, and 4.10 ± 0.10 cm, respectively, while root lengths improved to 1.53 ± 0.05 cm, 3.93 ± 0.63 cm, and 3.53 ± 0.05 cm, as shown in Table 3.

Table 3. The phytotoxic effect of decolorized dye product by *Pantoea dispersa* MS 3 on root and shoot length of *Vigna radiata* L. under azo dye stress conditions

Treatment	Dk Red RB		Blue GSL		Scarlet RR	
	Root Length (cm)	Shoot Length (cm)	Root Length (cm)	Shoot Length (cm)	Root Length (cm)	Shoot Length (cm)

Water Control	2.26±0.03[a]	3.22±0.02[a]	6.61±0.01[a]	9.25±0.04[a]	4.3±0.26[a]	5.4±0.36[a]
Dye Control	1.23±0.04[c]	1.64±0.04[c]	2.46±0.02[c]	4.15±0.04[c]	2.56±0.11[c]	2.03±0.15[c]
***Pantoea dispersa* MS 3**	1.53±0.05[b]	2.66±0.15[b]	3.93±0.63[b]	6.63±0.25[b]	3.53±0.05[b]	4.1±0.1[b]

Values are mean ± standard deviation of root and shoot length of *V. radiata* L. seeds under water control, dye control, and bacterial-treated conditions using DK. Red RB, Blue GSL, Scarlet RR dyes. Different alphabetic letters within the same column shows significant differences ($p < 0.05$) according to Tukey's HSD test following One-way ANOVA analysis.

Discussion

The successful isolation of 15 bacterial colonies with distinct morphology from textile-contaminated soil is consistent with previous research that indicates microorganisms from dye-polluted environments have specific adaptations and are therefore potential candidates for bioremediation of toxic wastewater (Meerbergen et al. 2018a). The formation of clear zones (halo zones) around isolates such as MS 3 on solid media containing dyes is a well-established indicator of extracellular enzymatic activity or a metabolic potential to decolorize azo bonds (Kishor, Purchase, et al. 2021a).

Dye degradation assay

Many microorganisms are used in biological approaches, including bacteria, fungi, yeasts, actinomycetes, and algae; however, bacteria are considered the most efficient wastewater treatment agents due to their rapid growth rate, exceptional adaptability to the environment, and extensive biochemical abilities (Garg, Garg, and Mukherji 2020; Kishor et al. 2020). The result suggests enzymatic activity, possibly including enzymes such as laccases, lignin peroxidase, and azoreductase (Kishor, Saratale, et al. 2021; Moyo, Makhanya, and Zwane 2022). The dye removal efficiency is influenced not only by microbial enzymatic capacity but also by the structural complexity and substituent groups of the azo dyes (R. L. Singh, Singh, and Singh 2015). The position of aromatic rings, the number of azo bonds (e.g., diazo vs. monoazo), and the presence of sulfonic acid groups of the dye can affect the susceptibility to enzyme degradation (Meerbergen et al. 2018a; Zahran et al. 2019).

Molecular identification

Molecular characterization identified the highly efficient dye-degrading isolate MS 3 as belonging to the genus *Pantoea*, a group increasingly acknowledged for their metabolic versatility and biodegradation capabilities in contaminated environments. The identification of *Pantoea dispersa* as a strain that can concurrently degrade dye and promote plant growth underlines its ecological importance and potential usage in sustainable bioremediation systems (Manikandan et al. 2025).

Analytical analysis

Untreated azo dye exhibited characteristic, intense absorption peaks associated with delocalized electron systems that are responsible for dye stability and chromatic intensity. Following bacterial treatment, significant attenuation of these peaks was observed, indicating enzymatic cleavage of chromophoric azo bonds and subsequent dye degradation (Zafar et al. 2022). In the UV–Vis region, a completely disappeared major adsorption peak or a new major adsorption peak indicates dye decolorization or degradation of color, a primary target of bacterial enzyme

activity (Ghafoor et al. 2024). This enzymatic reduction of the azo bond cleaves it into colorless aromatic amines, thereby resulting in significant decolorization. The observed decrease in λmax peak intensity aligns with previous reports demonstrating that microbial degradation of azo dyes is typically initiated via reductive cleavage of the -N=N- bond under enzymatic mediation (Zafar et al. 2022). In the present study, significant attenuation of absorbance peaks due to microbial decolorization leads to confirmation of effective decolorization and dye breakdown, as shown in Figure 3. The attenuation of the major absorption peaks or the emergence of a new peak in the UV region substantiates the formation of intermediate metabolites or further transformation products (Sreedharan, Saha, and Rao 2021). The reduction in absorbance among these different azo dyes highlights the broad substrate specificity and metabolic versatility of *P. dispersa* MS 3, suggesting its potential applicability for treating complex effluents containing multiple dye contaminants.

TLC analysis showed a single intact band in the untreated dye sample; such single-band patterns are consistent with an intact chromophoric system and have been widely reported for undegraded azo dyes, reflecting their homogeneous molecular composition and stability under non-biological conditions (Ajaz et al., 2019b). The occurrence of several chromatographic band with different Rf values indicates progressive decolorization and transformation of dye molecules into compounds with different polarity. In many studies, the control azo dye sample showed a single band with a single Rf value, indicating it behaves as one dominant and complex compound. In the TLC chromatogram of a decolorized Direct Orange 16 sample treated with *Micrococcus luteus* strain SSN2, Singh et al. (2015) detected two additional bands with Rf values of 0.63 and 0.965 when exposed to UV light at 254 nm. On the other hand, the untreated dye showed a single band with an Rf value of 0.74 (S. Singh et al. 2015). According to several previous studies, thin-layer chromatography (TLC) confirms the biotransformation of azo dyes in treated samples by bacterial isolates, since the parent dye band disappears and multiple new bands are observed, indicating bacterial transformation of the parent dye molecules into multiple transformation products . According to previous studies, bacteria express various enzymes like azoreductase, laccase, peroxidases, dehydrogenases, oxygenase, which cleave the azo bond and then modify the fragments (desulfonation, ring cleavage, oxidation), leading to the generation of several transformation products with different chromatographic characteristics. As metabolites have different polarity and structure, the degraded sample shows multiple bands (Ajaz et al. 2019d; Srinivasan, Bankole, and Sadasivam 2022a).

The FTIR spectra of the untreated azo dyes showed a prominent absorption band around 1650 cm^{-1}, along with bands corresponding to hydroxyl/amine, aliphatic C–H, aromatic, and sulfonic group-associated vibrations. Although the absorption band around 1650 cm^{-1} is often linked to vibrations of azo dye chromophores in earlier research (Adeniyi et al. 2023; Srinivasan et al. 2022a), this region may also consist of overlapping vibrations, indicating other functional groups such as C=C, C=O, and C=N stretching vibrations. FTIR spectral alterations strongly supported the chemical transformation of the dye structure following bacterial treatment. The -N=N- and sulfonated/aromatic functional groups in control azo dyes have been reported for methyl red, methyl orange,

Orange II, and Reactive Black 5 (Haque et al. 2021; Ikram et al. 2022a; Kaur et al. 2023; Khan et al. 2022). Additionally, broad peaks in the range of 3317- 3324 cm^{-1} corresponded to O-H or N-H stretching vibrations, while the peaks observed between 2944-2831 cm^{-1} were attributed to C-H stretching of aliphatic groups (Figure 5). Peaks in the region of 1448-1405 cm^{-1} were associated with C=C stretching of aromatic rings or C=O vibrations, and those in the range of 1112-1020 cm^{-1} were attributed to C-N stretching and sulfonic/sulfoxide group vibrations (Haque et al. 2021; Khan et al. 2022; Srinivasan, Bankole, and Sadasivam 2022b). After decolorization, significant alteration in the FTIR spectra was observed, indicating chemical transformation of the dye molecules. The azo specific peak, initially observed around 1650 cm^{-1}, appeared at 1658 cm^{-1} (Dk. Red RB), 1637 cm^{-1} (Blue GSL), and 1655 cm^{-1} (Scarlet RR) in the spectra of the sample treated with *P. dispersa* MS 3 (Figure 5); however, it either disappeared or showed a substantial reduction in intensity after decolorization, suggesting structural modification of the dye chromophore following bacterial treatment (Ikram et al. 2022a). Furthermore, the attenuation or shifting of bands in 1112–1020 cm^{-1} region suggests modification of sulfonate and aromatic group-associated functional groups (Haque et al. 2021). As a result of microbial decolorization, these spectral changes indicated that the parental dyes were broken down into simpler, less complex compounds. These observations align with earlier reports. FTIR analysis of untreated Reactive Red 22 shows a broad peak at 3444.87 $cm^{-1,}$ indicating -OH and $-NH_3$ interactions, with azo (-N=N-) and C-C=C asymmetric stretching at 1631.78 cm^{-1} and 1400.32 cm^{-1}, respectively. After degradation by *Bacillus infantis* strain AAA, the -OH and $-NH_3$ peaks appeared separately at 3464.15 and 4315.93 cm^{-1}, the azo peak disappeared, and the C=C stretch shifted to 1398.39 cm^{-1}, confirming azo bond cleavage (Bhaskara Rao, Arun Prasad, and Author 2014).

The biotransformation of Dk. Red RB, Blue GSL, and Scarlet RR by *P. dispersa* MS 3 is initiated by enzymatic cleavage of the azo -N=N- bond, as evident by a decrease in λmax in UV-Vis spectra and alterations in the FTIR profile. Attenuation of the single band on TLC and the appearance of 5-6 new bands with different Rf values for each dye indicate the presence of several intermediates with varying polarity and size. These intermediates are further subjected to oxidative degradation mediated by enzymes such as laccases and oygenases, leading to cleavage of aromatic rings (Srinivasan et al. 2022a). Although UV-Vis spectroscopy, TLC, and FTIR analyses demonstrated decolorization and structural transformation of the azo dyes following treatment, these techniques do not permit definite identification of degradation metabolites or confirmation of complete mineralization. Therefore, advanced analytical techniques such as LC-MS, GC-MS, or HPLC are recommended in future studies to characterize transformation products and evaluate the extent of detoxification.

Plant Growth-Promoting Traits

In addition to its degradative capability, the presence of PGP traits indicates the strain possesses significant potential to enhance plant growth. Such multifunctional attributes are particularly advantageous in dye-contaminated environments, where simultaneous pollutant remediation and restoration of plant productivity are critical.

Qualitative plate assays on N-free media are widely used as an initial screen for diazotrophic plant growth-promoting bacteria before more detailed physiological or molecular confirmation (Timofeeva, Galyamova, and Sedykh 2023). Nitrogen fixation is a pivotal trait for bacterial plant growth promotion, as it provides a supplementary nitrogen source in nutrient-depleted and contaminated soils. Previous studies have reported similar nitrogen-fixing ability of *Pantoea* spp., emphasizing their potential to enhance crop nitrogen nutrition (R et al. 2023a; Tariq et al. 2023). The growth of the *P. dispersa* MS3 on N-free Jensen media suggests its potential for fixing nitrogen and supports its possible role as a plant growth-promoting bacterium. However, further confirmation using molecular or biochemical approaches would be required to verify its nitrogen-fixing capability.

Bacterial phosphate solubilization is a key process that converts insoluble soil phosphates into forms that plants can absorb, supporting plant growth and sustainable agriculture. Phosphate-solubilizing bacteria (PSB) achieve this mainly by secreting organic acids and enzymes, making phosphorus more accessible to plants (Rawat et al. 2020). According to previous reports, plant growth promoters and phosphate solubilizers *Pantoea dispersa* spp. offer multiple benefits including improved nutrient uptake, yield, and soil health. It can sustainably increase agricultural yield when used as biofertilizers, particularly in extreme environments (Cui et al. 2023; Priya et al. 2022; R et al. 2023a; Rawat et al. 2022). Interestingly, a prior study found that *P. dispersa* FC-1 considerably increased phosphate solubilization, ranging from 160.79 to 270.22 mg/L when evaluated with four distinct insoluble phosphate sources (Cui et al. 2023).

Plant hormone Indole-3-acetic acid (IAA) is produced by many bacteria, including *Pantoea dispersa*, and plays a major role in promoting plant growth. In recent studies, *Pantoea dispersa* was shown to produce IAA efficiently, which improves root development, nodulation, and crop yield (Etesami and Glick 2024; Lv et al. 2022; Tariq et al. 2023). In our experiment, quantitative analysis showed that *P. dispersa* MS 3 produced a large amount of IAA, with a value of 44.74 (± 0.94) µg/mL. Previously, *Pantoea dispersa* strain MCA19 isolated from chickpea root nodules produced IAA at a concentration of 10.25 µg/mL. A significant increase in biomass accumulation and productivity was observed in chickpea plants after its application, with dry weights increasing by 30% and grain yields increasing by 38%. The increased root development and nutrient absorption were partially attributed to IAA-mediated effects (Tariq et al. 2023).

Since %SU in the CAS assay reflects the relative capacity to chelate Fe (III) from the CAS-Fe complex (Arora and Verma 2017), the 68.6 (±0.20) %SU recorded for *P. dispersa* MS3 indicates strong iron-chelating potential. Such high siderophore output is widely recognized as an important plant growth-promoting mechanism, improving Fe bioavailability to plants, especially in calcareous or contaminated soil where iron solubility is low (Maheshwari, Bhutani, and Suneja 2019).

The substantial GA3 production recorded in the present study further supports the PGP capability of *P. dispersa* MS 3. According to previous reports gibberellin production by strains of *Pantoea dispersa* has been demonstrated to improve plant growth and seed germination (Lv et al. 2022). The observed GA_3 production in the present study is

comparable to previous reported value for *Pantoea* spp. which have been shown to enhance plant growth and stress tolerance through multiple biochemical pathways (Ghosh et al. 2025). Laboratory studies have found that *Pantoea dispersa* SOB2 strains produce significant gibberellic acid (e.g., 162.266 g/mL), which is higher than many other beneficial bacteria (Nandni et al. 2025).

The combination of PGP traits exhibited by *P. dispersa* MS 3 highlights its potential as a multifunctional bacterial isolate for plant growth promotion and azo dye decolorization under controlled laboratory conditions.

Phytotoxicity assessment of decolorized product

The selection of *Vigna radiata* L. as the experimental plant further strengthens the phytotoxicity assessment because its rapid germination and high sensitivity to environmental pollutants enable reliable detection of both toxic and detoxified dye products. Its standardized growth metric provided a rigorous quantitative framework to validate the results (Pandey et al. 2024). A reduction in germination rates as well as seedling growth under untreated dye stress confirms the phytotoxic nature of azo dyes towards *Vigna radiata* L. A similar inhibitory effect of reactive and disperse dyes on mung bean growth was reported previously, with dye exposure reducing germination percentage and seedling vigor, and suppressing radicle and plumule development. The findings support the hypothesis that textile dyes disrupt cellular metabolism, inhibit water uptake, and cause oxidative stress in germinating seeds (Amin et al. 2020; Sompark, Damrianant, and Sakkayawong 2024). Furthermore, the reduction in inhibition percentage after bacterial treatment indicates that *P. dispersa* MS 3 mitigated the harmful effects of dye exposure. As a result of the microbe-assisted remediation, seedling germination and growth improved, consistent with earlier reports showing that dye toxicity can be reduced and plants can be more tolerant of contaminated environments (Amin et al. 2020; Moyo et al. 2022). Numerous plant growth-promoting traits, including as nutrient solubilization, nitrogen fixation, ammonia synthesis, ACC deaminase activity, and phytohormone production, are known to be expressed by plant-associated species of the genus *Pantoea.* These properties can all enhance plant development under stressful circumstances. Recent studies have demonstrated that Pantoea-based inoculation can enhance stress resilience and improve plant performance under toxic environmental conditions by reducing oxidative damage and promoting physiological stability (Manikandan et al. 2025; R et al. 2023b). Economically, *Pantoea dispersa* is a rhizosphere-associated bacterium widely distributed in diverse terrestrial environments, where it contributes to promoting nutrient cycling, plant-microbial interaction, and soil health. In addition to promoting plant growth, certain *Pantoea* strains possess the ability to degrade xenobiotic compound, including azo dyes, thereby supporting the restoration of contaminated environments (Coutinho and Venter 2026; Yang, Yi, and Xia 2023). However, since certain species within the genus have been identified as potential plant or human pathogens, it is crucial to conduct thorough biosafety assessments of specific strains prior to widespread use in environmental or agricultural settings (Yang et al. 2023).

Conclusion

This research successfully identifies *Pantoea dispersa* MS 3 as a versatile bacterial isolate for the integrated management of textile dye pollution. The isolate demonstrated high metabolic efficiency, achieving over 89% decolorization across three distinct azo dyes, with the most significant result recorded for Scarlet RR (92.07%). The biotransformation process, confirmed through a multi-analytical approach (UV-Vis, TLC, and FTIR), involves enzymatic cleavage of the azo bond, leading to the detoxification of the effluent. In addition to dye decolorization, *P. dispersa* MS 3 exhibited multiple plant growth-promoting traits, including nitrogen fixation, phosphate solubilization, IAA production, siderophore production, and GA3 production, highlighting its multifunctional potential as a beneficial rhizobacterium. The phytotoxicity assay further revealed that untreated azo dyes significantly inhibited seed germination and seedling growth of *Vigna radiata* L., whereas bacterial treatment considerably reduced dye toxicity and improved plant growth parameters.

Overall, the finding indicates that *P. dispersa* MS 3 can serve as an efficient and eco-friendly candidate for the bioremediation of azo-contaminated environment while simultaneously promoting plant growth under stress conditions. This study highlights the potential application of a multifunctional bacterial strain in sustainable wastewater treatment and agricultural rehabilitation. However, further studies are required to evaluate its performance in actual textile wastewater and under field conditions, together with comprehensive biosafety and metabolite analyses, before large-scale environmental application.

Acknowledgements

The authors extend their sincere gratitude to Uka Tarsadia University, Bardoli, for providing the essential facilities and resources that contributed to the successful completion of this research project.

Author contributions

Conceptualization and design of the study were contributed by all authors. Material preparation, data collection, experiments, analysis and the first draft were authored by Pimpalse Mohini. Conceptualization, validation, methodology, supervision, review, and editing were all contributed by the corresponding author, Dr. Naga Rathna Supriya. Review and editing were done by Vivek Patel, a co-author. Final approval of the manuscript was obtained from all authors.

Funding

The authors declare that no funds, grants, or other support were received during the preparation of this manuscript.

References:

Adeniyi, Adedeji Olumide, D. E. A. Boyro, Istifanus Yarkasuwa Chindo, and A. A. Mahmoud. 2023. "Spectrophotometric and Infra-Red Analyses of Azo Reactive Dyes Derived from 2-Methyl-3-(2'-Methylphenyl)-6-Arylazo-4- Oxoquinazoline." *Science World Journal* 18(2):231–39. doi:10.4314/SWJ.V18I2.10.

Ajaz, Mehvish, Abdul Rehman, Zaman Khan, Muhammad Atif Nisar, and Syed Hussain. 2019a. "Degradation of Azo Dyes by Alcaligenes Aquatilis 3c and Its Potential Use in the Wastewater Treatment." *AMB Express* 9(1):1–12. doi:10.1186/S13568-019-0788-3/FIGURES/7.

Ajaz, Mehvish, Abdul Rehman, Zaman Khan, Muhammad Atif Nisar, and Syed Hussain. 2019b. “Degradation of Azo Dyes by Alcaligenes Aquatilis 3c and Its Potential Use in the Wastewater Treatment.” *AMB Express* 9(1):1–12. doi:10.1186/S13568-019-0788-3/FIGURES/7.

Ajaz, Mehvish, Abdul Rehman, Zaman Khan, Muhammad Atif Nisar, and Syed Hussain. 2019c. “Degradation of Azo Dyes by Alcaligenes Aquatilis 3c and Its Potential Use in the Wastewater Treatment.” *AMB Express* 9(1):1–12. doi:10.1186/S13568-019-0788-3/FIGURES/7.

Ajaz, Mehvish, Abdul Rehman, Zaman Khan, Muhammad Atif Nisar, and Syed Hussain. 2019d. “Degradation of Azo Dyes by Alcaligenes Aquatilis 3c and Its Potential Use in the Wastewater Treatment.” *AMB Express* 9(1):1–12. doi:10.1186/S13568-019-0788-3/FIGURES/7.

Amin, Shivani, Rajesh Prasad Rastogi, Mukesh Ghanshyam Chaubey, Kunal Jain, Jyoti Divecha, Chirayu Desai, and Datta Madamwar. 2020. “Degradation and Toxicity Analysis of a Reactive Textile Diazo Dye-Direct Red 81 by Newly Isolated Bacillus Sp. DMS2.” *Frontiers in Microbiology* 11:576680. doi:10.3389/FMICB.2020.576680/BIBTEX.

Amri, Marwa, Mohamed Ridha Rjeibi, Marwa Gatrouni, Dina M. R. Mateus, Nedra Asses, Henrique J. O. Pinho, and Chaabane Abbes. 2023. “Isolation, Identification, and Characterization of Phosphate-Solubilizing Bacteria from Tunisian Soils.” *Microorganisms 2023, Vol. 11, Page 783* 11(3):783. doi:10.3390/MICROORGANISMS11030783.

Arora, Naveen Kumar, and Maya Verma. 2017. “Modified Microplate Method for Rapid and Efficient Estimation of Siderophore Produced by Bacteria.” *3 Biotech 2017 7:6* 7(6):381-. doi:10.1007/S13205-017-1008-Y.

Barua, Suman, Sohag Miah, M. Nuruddin Mahmud, and Ismail M. M. Rahman. 2023. “Isolation and Identification of Naturally Occurring Textile Effluent-Degrading Bacteria and Evaluation of Their Ability to Inhibit Potentially Toxic Elements.” *Results in Engineering* 17. doi:10.1016/J.RINENG.2023.100967.

Bhaskara Rao, K. V, A. S. Arun Prasad, and Corresponding Author. 2014. “Toxicity Assessment.” 13:369–74. www.neptjournal.com.

Biruntha, M., J. Archana, K. Kavitha, K. Vanimuthu, B. Karunai Selvi, J. Arockia John Paul, R. M. Vithyavathy, K. Kaviyarasu, and G. Ramalingam. 2021. “Efficacy of Dye Degradation of Contaminated Soil Microbial Isolates.” *Materials Today: Proceedings* 36:167–70. doi:10.1016/J.MATPR.2020.02.692.

Biswas, Shreya, Tuhin Kahali, Anwesha Mukherjee, Debasmita Chakraborty, Chayan Guha, Tathagata Adhikary, Pratik Das, Nandan Kumar Jana, Suvendu Manna, and Piyali Basak. 2024. “Enzymes Analysis, Degradation Kinetics, Response Surface Optimization and Heavy Metal Tolerance of the Biodegradation of Malachite Green by Stenotrophomonas Koreensis.” *Bioremediation Journal* 28(2):133–55. doi:10.1080/10889868.2022.2143472;JOURNAL:JOURNAL:BBRM20;PAGE:STRING:ARTICLE/CHAPTER.

Chachaty, Elisabeth, and Patrick Saulnier. 2000. “Isolating Chromosomal DNA from Bacteria.” *Nucleic Acid Protocols Handbook, The* 29–32. doi:10.1385/1-59259-038-1:29.

Cui, Ying, Yujie Zhao, Run Cai, Hao Zhou, Jiaxin Chen, Lirong Feng, Changhong Guo, and Dan Wang. 2023. “Isolation and Identification of a Phosphate-Solubilizing Pantoea Dispersa with a Saline–Alkali Tolerance and Analysis of Its Growth-Promoting Effects on Silage Maize Under Saline–Alkali Field Conditions.” *Current Microbiology* 80(9):1–13. doi:10.1007/S00284-023-03408-8/METRICS.

Etesami, Hassan, and Bernard R. Glick. 2024. “Bacterial Indole-3-Acetic Acid: A Key Regulator for Plant Growth, Plant-Microbe Interactions, and Agricultural Adaptive Resilience.” *Microbiological Research* 281:127602. doi:10.1016/J.MICRES.2024.127602.

Garg, Neha, Anurag Garg, and Suparna Mukherji. 2020. “Eco-Friendly Decolorization and Degradation of Reactive Yellow 145 Textile Dye by Pseudomonas Aeruginosa and Thiosphaera Pantotropha.” *Journal of Environmental Management* 263:110383. doi:10.1016/J.JENVMAN.2020.110383.

Ghafoor, Sidra, Eeman Ali, Fazal Rahim, Dilara Abbas Bukhari, Shaista Shafiq, Syed Zajif Hussain, and Abdul Rehman. 2024. “Evaluation of Azo Dyes Degradation Potential of Aspergillus Strains: A Strategy for Waste Management.” *Journal of Hazardous Materials Advances* 16:100475. doi:10.1016/J.HAZADV.2024.100475.

Ghosh, Sudip Kumar, Pallab Kumar Ghosh, Priyanka Pal, Sayanta Mondal, and Tushar Kanti Maiti. 2025. "Unveiling the Role of Salt Tolerant Pantoea Dispersa MCC 3879 in Enhancing Salinity Resilience and Promoting Seedling Growth of Rice (Oryza Sativa L.) Genotypes through Cellular Osmotic, Ionic, and Redox Homeostasis." *Biocatalysis and Agricultural Biotechnology* 69:103811. doi:10.1016/J.BCAB.2025.103811.

Gordon, S. A., and L. G. Paleg. 1957. "Observations on the Quantitative Determination of Indoleacetic Acid." *Physiologia Plantarum* 10(1):39. doi:10.1111/J.1399-3054.1957.TB07608.X.

Grimm, Phyllis Weisel, and Paul J. Allen. 1954. "Promotion by Zinc of the Formation of Cytochromes in Ustilago Sphaerogena." *Plant Physiology* 29(4):369. doi:10.1104/PP.29.4.369.

Haque, Md Manjurul, Md Amdadul Haque, Md Khaled Mosharaf, and Polash Kisku Marcus. 2021. "Decolorization, Degradation and Detoxification of Carcinogenic Sulfonated Azo Dye Methyl Orange by Newly Developed Biofilm Consortia." *Saudi Journal of Biological Sciences* 28(1):793–804. doi:10.1016/J.SJBS.2020.11.012.

HOLBROOK, ALLAN A., W. J. W. EDGE, and FRED BAILEY. 1961. "Spectrophotometric Method for Determination of Gibberellic Acid." 159–67. doi:10.1021/BA-1961-0028.CH018.

Ikram, Muhammad, Mohammad Naeem, Muhammad Zahoor, Abdur Rahim, Marlia Mohd Hanafiah, Adeleke Abdulrahman Oyekanmi, Abdul Bari Shah, Mater H. Mahnashi, Amer Al Ali, Naif A. Jalal, Farkad Bantun, and Abdul Sadiq. 2022a. "Biodegradation of Azo Dye Methyl Red by Pseudomonas Aeruginosa: Optimization of Process Conditions." *International Journal of Environmental Research and Public Health 2022, Vol. 19, Page 9962* 19(16):9962. doi:10.3390/IJERPH19169962.

Ikram, Muhammad, Mohammad Naeem, Muhammad Zahoor, Abdur Rahim, Marlia Mohd Hanafiah, Adeleke Abdulrahman Oyekanmi, Abdul Bari Shah, Mater H. Mahnashi, Amer Al Ali, Naif A. Jalal, Farkad Bantun, and Abdul Sadiq. 2022b. "Biodegradation of Azo Dye Methyl Red by Pseudomonas Aeruginosa: Optimization of Process Conditions." *International Journal of Environmental Research and Public Health* 19(16). doi:10.3390/IJERPH19169962.

Jensen, H. L. 1955. "Azotobacter Macrocytogenes n. Sp., a Nitrogen-Fixing Bacterium Resistant to Acid Reaction." *Acta Agriculturae Scandinavica* 5(1):280–94. doi:10.1080/00015125509441446/ASSET//CMS/ASSET/B60A9DB6-41DD-4922-BB24-800E1422B3AF/00015125509441446.FP.PNG.

Joshi, Gajendra, Vikash Kumar, and Sunil Kumar Brahmachari. 2021. "Screening and Identification of Novel Halotolerant Bacterial Strains and Assessment for Insoluble Phosphate Solubilization and IAA Production." *Bulletin of the National Research Centre 2021 45:1* 45(1):1–12. doi:10.1186/S42269-021-00545-7.

Kalyan, V. S. Reddy Kiran, S. Meena, S. Karthikeyan, and D. Jawahar. 2022. "Isolation, Screening, Characterization, and Optimization of Bacteria Isolated from Calcareous Soils for Siderophore Production." *Archives of Microbiology* 204(12):1–13. doi:10.1007/S00203-022-03322-W/METRICS.

Kamal, Islam M., Nourtan F. Abdeltawab, Yasser M. Ragab, Mohamed A. Farag, and Mohammed A. Ramadan. 2022. "Biodegradation, Decolorization, and Detoxification of Di-Azo Dye Direct Red 81 by Halotolerant, Alkali-Thermo-Tolerant Bacterial Mixed Cultures." *Microorganisms* 10(5):994. doi:10.3390/MICROORGANISMS10050994/S1.

Kaur, Jaspreet, Gaurav Mudgal, Arvind Negi, Jeewan Tamang, Shambhawi Singh, Gajendra Bahadur Singh, Jagadeesh Chandra Bose K, Sandip Debnath, Mohammad Ahmad Wadaan, Muhammad Farooq Khan, Janne Ruokolainen, and Kavindra Kumar Kesari. 2023. "Reactive Black-5, Congo Red and Methyl Orange: Chemical Degradation of Azo-Dyes by Agrobacterium." *Water (Switzerland)* 15(9):1664. doi:10.3390/W15091664/S1.

Khan, Arshiya, Anuraj Nayarisseri, and Sanjeev Kumar Singh. 2025. "Characterization and Optimization of Azo Dyes Degrading Microbes Isolated from Textile Effluent." *Scientific Reports* 15(1):1–23. doi:10.1038/S41598-025-95359-2;SUBJMETA=114,1647,326,61,631;KWRD=BIOLOGICAL+TECHNIQUES,BIOTECHNOLOGY,COMPUTATIONAL+BIOLOGY+AND+BIOINFORMATICS,MICROBIOLOGY.

Khan, Asad Ullah, Muhammad Zahoor, Mujaddad Ur Rehman, Abdul Bari Shah, Ivar Zekker, Farhat Ali Khan, Riaz Ullah, Ghadeer M. Albadrani, Roula Bayram, and Hanan R. H. Mohamed. 2022. "Biological Mineralization of Methyl Orange by Pseudomonas Aeruginosa." *Water 2022, Vol. 14, Page 1551* 14(10):1551. doi:10.3390/W14101551.

Kishor, Roop, Diane Purchase, Luiz Fernando Romanholo Ferreira, Sikandar I. Mulla, Muhammad Bilal, and Ram Naresh Bharagava. 2020. “Environmental and Health Hazards of Textile Industry Wastewater Pollutants and Its Treatment Approaches.” *Handbook of Environmental Materials Management* 1–24. doi:10.1007/978-3-319-58538-3_230-1.

Kishor, Roop, Diane Purchase, Ganesh Dattatraya Saratale, Luiz Fernando Romanholo Ferreira, Muhammad Bilal, Hafiz M. N. Iqbal, and Ram Naresh Bharagava. 2021a. “Environment Friendly Degradation and Detoxification of Congo Red Dye and Textile Industry Wastewater by a Newly Isolated Bacillus Cohnni (RKS9).” *Environmental Technology and Innovation* 22. doi:10.1016/J.ETI.2021.101425.

Kishor, Roop, Diane Purchase, Ganesh Dattatraya Saratale, Luiz Fernando Romanholo Ferreira, Muhammad Bilal, Hafiz M. N. Iqbal, and Ram Naresh Bharagava. 2021b. “Environment Friendly Degradation and Detoxification of Congo Red Dye and Textile Industry Wastewater by a Newly Isolated Bacillus Cohnni (RKS9).” *Environmental Technology & Innovation* 22:101425. doi:10.1016/J.ETI.2021.101425.

Kishor, Roop, Ganesh Dattatraya Saratale, Rijuta Ganesh Saratale, Luiz Fernando Romanholo Ferreira, Muhammad Bilal, Hafiz M. N. Iqbal, and Ram Naresh Bharagava. 2021. “Efficient Degradation and Detoxification of Methylene Blue Dye by a Newly Isolated Ligninolytic Enzyme Producing Bacterium Bacillus Albus MW407057.” *Colloids and Surfaces B: Biointerfaces* 206:111947. doi:10.1016/J.COLSURFB.2021.111947.

Lv, Luqiong, Jinyan Luo, Temoor Ahmed, Haitham E. M. Zaki, Ye Tian, Muhammad Shafiq Shahid, Jianping Chen, and Bin Li. 2022. “Beneficial Effect and Potential Risk of Pantoea on Rice Production.” *Plants 2022, Vol. 11, Page 2608* 11(19):2608. doi:10.3390/PLANTS11192608.

Maheshwari, Rajat, Namita Bhutani, and Pooja Suneja. 2019. “Screening and Characterization of Siderophore Producing Endophytic Bacteria from Cicer Arietinum and Pisum Sativum Plants.” doi:10.7324/JABB.2019.70502.

Manikandan, Soumya Koippully, Attiat Elnaggar, Islam M. Ahmady, François Mitterand Tsombou, Khaled A. El-Tarabily, Mohamed S. Sheteiwy, and Ali El-Keblawy. 2025. “Endophytic Pantoea Agglomerans Enhances Lead Phytoremediation and Stress Resilience of Calotropis Procera in Hydroponic System.” *Scientific Reports* 15(1):26712. doi:10.1038/S41598-025-04558-4.

Meerbergen, Ken, Kris A. Willems, Raf Dewil, Jan Van Impe, Lise Appels, and Bart Lievens. 2018a. “Isolation and Screening of Bacterial Isolates from Wastewater Treatment Plants to Decolorize Azo Dyes.” *Journal of Bioscience and Bioengineering* 125(4):448–56. doi:10.1016/J.JBIOSC.2017.11.008.

Meerbergen, Ken, Kris A. Willems, Raf Dewil, Jan Van Impe, Lise Appels, and Bart Lievens. 2018b. “Isolation and Screening of Bacterial Isolates from Wastewater Treatment Plants to Decolorize Azo Dyes.” *Journal of Bioscience and Bioengineering* 125(4):448–56. doi:10.1016/J.JBIOSC.2017.11.008.

Moyo, Senelisile, Bukisile P. Makhanya, and Pinkie E. Zwane. 2022. “Use of Bacterial Isolates in the Treatment of Textile Dye Wastewater: A Review.” *Heliyon* 8(6):e09632. doi:10.1016/J.HELIYON.2022.E09632.

Nandni, Savita Rani, Indu Dhiman, and Leela Wati. 2025. “Biopriming with Multifarious Sulphur-Oxidizing Bacteria Improve in Vitro Vigna Radiata L. (Mung Bean) and Brassica Juncea L. (Mustard) Seed Germination.” *Folia Microbiologica* 70(2):427–39. doi:10.1007/S12223-024-01195-8/METRICS.

Nautiyal, C. Shekhar. 1999. “An Efficient Microbiological Growth Medium for Screening Phosphate Solubilizing Microorganisms.” *FEMS Microbiology Letters* 170(1):265–70. doi:10.1111/J.1574-6968.1999.TB13383.X.

Pandey, Akanksha, Vinay Mohan Pathak, Navneet, and Minakshi Rajput. 2024. “A Feasible Approach for Azo-Dye (Methyl Orange) Degradation by Textile Effluent Isolate Serratia Marcescens ED1 Strain for Water Sustainability: AST Identification, Degradation Optimization and Pathway Hypothesis.” *Heliyon* 10(11):e32339. doi:10.1016/J.HELIYON.2024.E32339.

Priya, P., B. Aneesh, K. C. Sivakumar, and K. Harikrishnan. 2022. “Comparative Proteomic Analysis of Saline Tolerant, Phosphate Solubilizing Endophytic Pantoea Sp., and Pseudomonas Sp. Isolated from Eichhornia Rhizosphere.” *Microbiological Research* 265:127217. doi:10.1016/J.MICRES.2022.127217.

Radhika, Birmole, and Aruna K. 2022. “ELUCIDATING A PATHWAY FOR DEGRADATION OF AZO DYE REACTIVE RED 120 BY BACTERIAL CONSORTIUM.” *Journal of Applied Biological Sciences* 16(3):396–417. doi:10.71336/JABS.1042.

Rani, Sushma, Anju Sogarwal, Gargi, Sonal Mishra, and Sahib Kaur. 2025. “Harnessing Plant-Bacterial Interactions to Enhance Abiotic Stress Tolerance in Plants: A Review.” *Discover Plants 2025 2:1* 2(1):250-. doi:10.1007/S44372-025-00330-0.

R, Aswani, Nejumal K. K, Sebastian K. S, C. T. Aravindakumar, and Radhakrishnan E. K. 2023a. “Plant Protection Mediated Through an Array of Metabolites Produced by Pantoea Dispersa Isolated from Pitcher Plant.” *Applied Biochemistry and Biotechnology* 195(3):1607–29. doi:10.1007/S12010-022-04179-X/METRICS.

R, Aswani, Nejumal K. K, Sebastian K. S, C. T. Aravindakumar, and Radhakrishnan E. K. 2023b. “Plant Protection Mediated Through an Array of Metabolites Produced by Pantoea Dispersa Isolated from Pitcher Plant.” *Applied Biochemistry and Biotechnology* 195(3):1607–29. doi:10.1007/S12010-022-04179-X.

Rawat, Pratibha, Sudeshna Das, Deepti Shankhdhar, and S. C. Shankhdhar. 2020. “Phosphate-Solubilizing Microorganisms: Mechanism and Their Role in Phosphate Solubilization and Uptake.” *Journal of Soil Science and Plant Nutrition 2020 21:1* 21(1):49–68. doi:10.1007/S42729-020-00342-7.

Rawat, Pratibha, Anita Sharma, Deepti Shankhdhar, and S. C. Shankhdhar. 2022. “Comparative Response of Phosphate Solubilizing Indigenous Bacillus Licheniformis, Pantoea Dispersa and Staphylococcus Sp. From Rice Rhizosphere for Their Multifarious Growth Promoting Characteristics.” *Geomicrobiology Journal* 39(6):445–52. doi:10.1080/01490451.2022.2027049;SUBPAGE:STRING:ABSTRACT;JOURNAL:JOURNAL:UGMB20;WGROUP:STRING:PUBLICATION.

Schwyn, Bernhard, and J. B. Neilands. 1987. “Universal Chemical Assay for the Detection and Determination of Siderophores.” *Analytical Biochemistry* 160(1):47–56. doi:10.1016/0003-2697(87)90612-9.

Shahid, Muhammad, Faisal Mahmood, Sabir Hussain, Tanvir Shahzad, Muhammad Zulqarnain Haider, Muhammad Noman, Aqsa Mushtaq, Qundeel Fatima, Temoor Ahmed, and Ghulam Mustafa. 2018. “Enzymatic Detoxification of Azo Dyes by a Multifarious Bacillus Sp. Strain MR-1/2-Bearing Plant Growth-Promoting Characteristics.” *3 Biotech* 8(10):1–12. doi:10.1007/S13205-018-1442-5/METRICS.

Sharma, Abhishek. 2018. “Extraction and Evaluation of Gibberellic Acid from Pseudomonas Sp.: Plant Growth Promoting Rhizobacteria.” *Article in International Research Journal of Pharmacy*. https://www.researchgate.net/publication/323445997.

Singh, Ram Lakhan, Pradeep Kumar Singh, and Rajat Pratap Singh. 2015. “Enzymatic Decolorization and Degradation of Azo Dyes – A Review.” *International Biodeterioration & Biodegradation* 104:21–31. doi:10.1016/J.IBIOD.2015.04.027.

Singh, S., S. Chatterji, P. T. Nandini, A. S. A. Prasad, and K. V. B. Rao. 2015. “Biodegradation of Azo Dye Direct Orange 16 by Micrococcus Luteus Strain SSN2.” *International Journal of Environmental Science and Technology* 12(7):2161–68. doi:10.1007/S13762-014-0588-X/METRICS.

Sompark, Chalermwoot, Somchit Damrianant, and Niramol Sakkayawong. 2024. “Phytotoxicity and Genotoxicity Study of Reactive Red 141 Dye on Mung Bean (Vigna Radiata (L.) Wilczek) Seedlings.” *Molecular Biology Reports* 51(1). doi:10.1007/S11033-023-08917-0.

Sreedharan, Veena, Purbasha Saha, and Kokati Venkata Bhaskara Rao. 2021. “Dye Degradation Potential of Acinetobacter Baumannii Strain VITVB against Commercial Azo Dyes.” *Bioremediation Journal* 25(4):347–68. doi:10.1080/10889868.2020.1871317.

Srinivasan, Shantkriti, Paul Olusegun Bankole, and Senthil Kumar Sadasivam. 2022a. “Biodecolorization and Degradation of Textile Azo Dyes Using Lysinibacillus Sphaericus MTCC 9523.” *Frontiers in Environmental Science* 10:990855. doi:10.3389/FENVS.2022.990855/BIBTEX.

Srinivasan, Shantkriti, Paul Olusegun Bankole, and Senthil Kumar Sadasivam. 2022b. “Biodecolorization and Degradation of Textile Azo Dyes Using Lysinibacillus Sphaericus MTCC 9523.” *Frontiers in Environmental Science* 10:990855. doi:10.3389/FENVS.2022.990855/BIBTEX.

Srinivasan, Shantkriti, and Senthil Kumar Sadasivam. 2018. “Exploring Docking and Aerobic-Microaerophilic Biodegradation of Textile Azo Dye by Bacterial Systems.” *Journal of Water Process Engineering* 22:180–91. doi:10.1016/J.JWPE.2018.02.004.

Srinivasan, Shantkriti, and Senthil Kumar Sadasivam. 2021. “Biodegradation of Textile Azo Dyes by Textile Effluent Non-Adapted and Adapted Aeromonas Hydrophila.” *Environmental Research* 194. doi:10.1016/J.ENVRES.2020.110643.

Suhag, Mahmudul Hassan, KM Anis Ul Haque, Md Zobaidul Hossen, Abul Kalam Azad, and Muhammad Younus. 2021. “Biodegradation of Azo Dyes and Dyes Present in Textile Wastewaters Using Bacillus Sp. Az28, Obtained from Industrial Effluents.” *Journal of Bangladesh Academy of Sciences* 45(1):117–22. doi:10.3329/JBAS.V45I1.54263.

Tariq, Mohsin, Nayab Hasnain, Ijaz Rasul, Muhammad Azeem Asad, Aqsa Javed, Kamran Rashid, Javeria Shafique, Wajeeha Iram, Amir Hameed, and Marriam Zafar. 2023. “Reconnoitering the Capabilities of Nodule Endophytic Pantoea Dispersa for Improved Nodulation and Grain Yield of Chickpea (Cicer Arietinum L.).” *World Journal of Microbiology and Biotechnology* 39(3):1–15. doi:10.1007/S11274-023-03525-3/METRICS.

Timofeeva, Anna M., Maria R. Galyamova, and Sergey E. Sedykh. 2023. “Plant Growth-Promoting Soil Bacteria: Nitrogen Fixation, Phosphate Solubilization, Siderophore Production, and Other Biological Activities.” *Plants 2023, Vol. 12, Page 4074* 12(24):4074. doi:10.3390/PLANTS12244074.

Wael, Dalia, Yasser El-Amier, Wesameldin I. A. Saber, and Ashraf Elsayed. 2024. “Plant-Associated Halotolerant Bacteria Improving Growth of Vicia Faba L. Mariout-2 under Salinity Conditions.” *Scientific Reports* 14(1):1–16. doi:10.1038/S41598-024-66504-0;SUBJMETA=172,326,449,61,631,704;KWRD=BIOTECHNOLOGY,ENVIRONMENTAL+SCIENCES,MICROBIOLOGY,PLANT+SCIENCES.

Weisburg, W. G., S. M. Barns, D. A. Pelletier, and D. J. Lane. 1991. “16S Ribosomal DNA Amplification for Phylogenetic Study.” *Journal of Bacteriology* 173(2):697–703. doi:10.1128/JB.173.2.697-703.1991.

Zafar, Sadia, Dilara A. Bukhari, and Abdul Rehman. 2022. “Azo Dyes Degradation by Microorganisms – An Efficient and Sustainable Approach.” *Saudi Journal of Biological Sciences* 29(12):103437. doi:10.1016/J.SJBS.2022.103437.

Zahran, Sara A., Marwa Ali-Tammam, Abdelgawad M. Hashem, Ramy K. Aziz, and Amal E. Ali. 2019. “Azoreductase Activity of Dye-Decolorizing Bacteria Isolated from the Human Gut Microbiota.” *Scientific Reports 2019 9:1* 9(1):1–14. doi:10.1038/s41598-019-41894-8.